João Victor B. Soares[1], Clodoaldo Valverde[1,2], André D. da Silva[1], Bruno V. Luz[1], Daniel Junior A. dos Santos[1], Elisa G. B. Carvalho[1], Yara Cecília M. Oliveira[1], Hamilton B. Napolitano[1], Basílio Baseia[3,4] Francisco A. P. Osório[4,5]

[1]Laboratório de Modelagem Molecular Aplicada e Simulação (LaMMAS), Campus de Ciências Exatas e Tecnológicas, Universidade Estadual de Goiás, 75001-970, Anápolis, GO, Brazil.
[2]Universidade Paulista – (UNIP), 74845-090, Goiânia, GO, Brazil.
[3]Departamento de Física, Universidade Federal da Paraíba, 58.051-970, João Pessoa, PB, Brazil.
[4]Instituto de Física, Universidade Federal de Goiás, 74.690-900, Goiânia, GO, Brazil
[5]Escola de Ciências Exatas e da Computação, Pontifícia Universidade Católica de Goiás, 74605-220, Goiânia, GO, Brazil.

***Correspondence author:** valverde@ueg.br

Received: 09/09/19. Approved: 20/11/19

Theoretical study of solvent effects on the hyperpolarizabilities of two chalcone derivatives

Abstract

The use of organic as nonlinear optical materials has been intensively explored in the recent years due to the ease of manipulation of the molecular structure and the synthetic flexibility regarding the change of substituent groups. In the present work, the linear and nonlinear properties of two chalcones derivatives (E)-1-(4-methylphenyl)-3-phenylprop-2-en-1-one (4MP3P) and (E)-1-(4-Nitrophenyl)-3-phenylprop-2-en-1-one (4NP3P), that differ by the substituent position at the phenyl ring, were studied in the presence of protic and aprotic solvents simulated by the Polarizable Continuum Model (PCM) at DFT/B3LYP/6-311+G(d) level. The static and dynamic (1064 nm) molecular parameters as the dipole moment, linear polarizability, first and second hyperpolarizabilities were studied as function of the solvent dielectric constant value. The geometrical behavior as the chemical bond angles, torsion angles, and partial charges distribution of the compounds were studied, including calculations of gap energies in various solvents. The obtained results revealed that the substituent change of CH_3 (4MP3P) to NO_2 (4NP3P) benefits the nonlinear optical properties of the compounds in the presence of the solvent media, the absolute values of the parallel first hyperpolarizability were the ones that present the greater variation.

Keywords: first and second hyperpolarizabilities; solvent; DMSO; acetone.

Estudio teórico de los efectos de solvente sobre la hiperpolarizabilidad de dos derivados de la chalcona

Resumen

El uso de materiales orgánicos como materiales ópticos no lineales se ha explorado intensamente en los últimos años, debido a la facilidad de manipulación de estas estructuras moleculares y la flexibilidad de síntesis en relación con el cambio de grupos sustituyentes. En el presente trabajo, las propiedades lineales y no lineales de dos derivados de chalcona (E)-1-(4-metilfenil)-3-fenilprop-2-en-1-ona (4MP3P) y (E)-1-(4-nitrofenil)-3-fenilprop-2-en-1-ona (4NP3P), los cuales difieren en la posición del sustituyente en el anillo de fenilo, se estudiaron en presencia de disolventes próticos y apróticos simulados por el Modelo Continuo Polarizable a nivel DFT/B3LYP/6-311+G(d). Además, se estudiaron parámetros moleculares estáticos y dinámicos (1064 nm) como el momento dipolar, la polarización lineal y la primera y la segunda hiperpolarización en función del valor constante dieléctrico del disolvente. El comportamiento geométrico se estudió como ángulos de enlace químico, ángulos de torsión y distribución de carga parcial de compuestos, incluidos los cálculos de energía de huecos en varios solventes. Los resultados mostraron que el cambio del sustituyente CH_3 (4MP3P) a NO_2 (4NP3P) beneficia las propiedades ópticas no lineales de los compuestos en presencia del medio solvente, los valores absolutos de la primera hiperpolarizabilidad paralela fueron los que presentaron la mayor variación.

Palabras clave: primera y segunda hiperpolarizabilidad; solvente; DMSO; acetona.

Estudo teórico dos efeitos do solvente nas hiperpolarizabilidades de dois derivados da chalcona

Resumo

O uso de materiais orgânicos como materiais ópticos não lineares tem sido intensamente explorado nos últimos anos, devido à facilidade de manipulação dessas estruturas moleculares e à flexibilidade de síntese em relação à mudança de grupos substituintes. No presente trabalho, as propriedades lineares e não lineares de dois derivados de chalconas (E)-1-(4-metilfenil)-3-fenilprop-2-en-1-ona (4MP3P) e (E)-1-(4-nitrofenil)-3-fenilprop-2-en-1-ona (4NP3P), que diferem pela posição do substituinte no anel fenil, foram estudados na presença de solventes próticos e apróticos simulados pelo Modelo Continuo Polarizável (PCM) no nível DFT/B3LYP/6-311+G(d). Os parâmetros moleculares estáticos e dinâmicos (1064 nm) como momento dipolar, polarizabilidade linear, primeira e segunda hiperpolarizabilidades foram estudados em função do valor da constante dielétrica do solvente. Estudou-se o comportamento geométrico como ângulos de ligação química, ângulos de torção e distribuição parcial de cargas dos compostos, incluindo cálculos de energias de gap em vários solventes. Os resultados obtidos revelaram que a mudança do substituinte de CH_3 (4MP3P) para NO_2 (4NP3P) beneficia as propriedades ópticas não lineares dos compostos na presença do meio solvente, os valores absolutos da primeira hiperpolarizabilidade paralela foram os que apresentaram a maior variação.

Palavras-chave: primeira e segunda hiperpolarizabilidades; solvente; DMSO; acetona.

Introduction

In the last few years the engineering of organic crystalline compound has become an important area of study and has attracted great interest from research centers [1], motivated by significant values of the nonlinear optical properties of these crystals, for instance, chalcone derivatives [2]. Nonlinear optics devices operate with high-speed information [3], as ultra-short pulse lasers, photonic devices, optical modulators, and others with applications in the areas of health and medicine [4, 5]. The advantages of organic crystals that have attracted much attention come from their ease of manipulation of the molecular structure and the synthetic flexibility regarding the change of substituent groups [6, 7]. The combination of the high nonlinearity characteristic of some organic compounds and the versatility of synthetic routes leads to maximization of the nonlinear optical properties [8]. Among the organic materials, the chalcones are known as promising compounds, since their derivatives have several biological properties that have been used as prototypes for new drugs [9]. Biosynthesis of flavonoids chalcones have been applied in several activities such as: antitumor [10], anti-inflammatory [11], antibacterial [12], antifungal [13], among others.

The chalcones consist of two aromatic rings joined by an unsaturated system so that their structure almost always acquires a linear or almost planar conformation [14]. Organic molecules with π-conjugated structures and donor and/or acceptor groups are compounds of great interest in the area of nonlinear optics [15]. The change of the substituent groups bond to the aromatic rings leads the chalcone molecules to acquire specific properties due the change of electronic distribution of the compound, hence new properties can be explored with each new substituent being added or substituted to the compound [16].

The purpose of the present paper is to study the nonlinear optical properties of two chalcone derivatives: (*E*)-1-(4-methylphenyl)-3-phenylprop-2-en-1-one (4MP3P) and (*E*)-1-(4-Nitrophenyl)-3-phenylprop-2-en-1-one (4NP3P), with formulas $C_{16}H_{14}O$ and $C_{15}H_{11}O_3$, respectively. The structure 4MP3P was synthesized by Toda *et al.* [15] and the structure 4NP3P by Jing *et al.* [16]. These compounds differ by the substituent at position 4 of the phenyl ring (B) as shown in Figure 1.

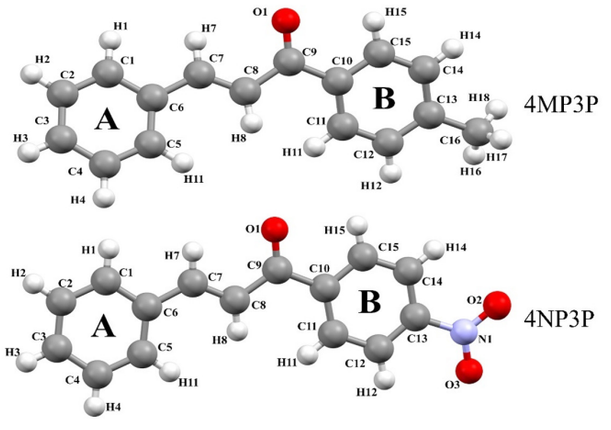

Figure 1. Molecular structure of the compounds 4MP3P and 4NP3P.

The electrical parameters of these compounds were calculated at DFT/CAM-B3LYP/6-311+G(d) level in the presence of several solvent media that are modeled by the Polarizable Continuum Model (PCM). The static and dynamic (1064 nm) molecular parameters as the dipole moment, linear polarizability, first and second hyperpolarizability were studied as function of the value of the solvent dielectric constant value. Also, the frontiers molecular orbital, HOMO (highest occupied molecular orbital) and LUMO (lowest unoccupied molecular orbital), and the respective gap energies in various solvents were calculated. The geometrical behavior of the compounds as the chemical bond angles, torsion angles, and partial charges distribution were also studied.

Materials and Methods

Computational procedures

Organic solvents belong to a class of liquid and volatile compounds and have the function of solubilizing, extracting, treating, and facilitating a chemical reaction among other functions. This group of compounds is divided into: polar and nonpolar solvents. Polar protic solvents are characterized by the presence of hydrogen bonded to electronegative elements, usually, atoms of O, N, and F, which can lead to the formation of hydrogen bonds [17] and polar aprotic solvents are characterized by the absence of electronegative atoms so that only bonds between carbon and hydrogen atoms are present. The values of the dielectric constant and of the dipole moments for polar solvents are higher than those for the nonpolar solvents [18]. The dielectric constant (ε) of a solvent medium is a good indicator of the ability to accommodate a charge separation that increases with the values of the dipole moment and with the polarizability of the molecule [19].

In this work the quantitative concept of the solvent polarity was considered through the normalized transition energy (E_T^N) scale of Dimroth and Reichardt [19, 20]. The E_T^N-value is based on the transition energy to the solvatochromic absorption band for the greatest wavelenght of the nitrile betaine pyridynium dye. Table 1 shows a list of the solvent media, here considered with the respective values of E_T^N and ε. Reactions involving charge separation in the E_T^N-scale advance more slowly in polar aprotic solvents due to the small dipole moments and the absence of hydrogen bonds which make them few effective in the development of the separation and the stabilization of charges when compared to the polar protic solvents[19, 21].

Table 1: Polarity of several solvent media following E_T^N-scale [22].

Solvents	E_T^N	ε	Type
Water	1.000	78.355	Protic
Methanol	0.762	32.613	Protic
Ethanol	0.654	24.852	Protic
DMSO	0.444	46.826	Aprotic
Acetone	0.355	20.493	Aprotic
Dichloroethane	0.327	10.125	Aprotic
Chloroform	0.259	4.711	nonpolar
Tetrahydrofuran	0.207	7.430	Aprotic
Heptane	0.012	1.911	nonpolar

The first two parameters are dimensionless.

Here the solvent chloroform must be considered nonpolar because the value of its dielectric constant ε is less than 5.

The total dipole moment and the average linear polarizability were calculated from the components x, y, and z, through the expressions:

$$\mu = \left(\mu_x^2 + \mu_y^2 + \mu_z^2\right)^{\frac{1}{2}} \qquad (1)$$

$$\langle\alpha\rangle = \frac{\alpha_{xx} + \alpha_{yy} + \alpha_{zz}}{3} \qquad (2)$$

The first hyperpolarizabilities considered concerned here were the parallel components to the direction of dipole moment (taken as z-direction) given by,

$$\beta_{||} = \frac{1}{5}\sum_{i=1}^{3}(\beta_{zii} + \beta_{izi} + \beta_{iiz}) \qquad (3)$$

and the Hyper-Rayleigh Scattering first hyperpolarizability (β_{HRS}) defined by,

$$\beta_{HRS} = \sqrt{\langle\beta^2_{ZZZ}\rangle + \langle\beta^2_{XZZ}\rangle} \qquad (4)$$

where the laboratory system of reference is adopted as *X*, *Y*, and *Z* coordinates. The *X*-direction is assumed as the fundamental light beam propagation, polarized in the *Z*-direction. The $\langle\beta^2_{ZZZ}\rangle$ and $\langle\beta^2_{XZZ}\rangle$ are macroscopic averages calculated from the first hyperpolarizability components (β_{ijk}) through the expressions,

$$\langle\beta^2_{ZZZ}\rangle = \frac{1}{210}(30\delta_1 + 12(\delta_2 + \delta_3 + \delta_5) + 6(\delta_4 + \delta_6) + 2(\delta_7 + \delta_8 + \delta_{11}) + 4\delta_9 + \delta_{10}),$$

$$\langle\beta^2_{XZZ}\rangle = \frac{1}{210}(6(\delta_1 - \delta_3 - \delta_5 + \delta_7) + 8\delta_2 + 18\delta_4 + 4\delta_6 - \delta_8 - 2\delta_9 + 3\delta_{10} - \delta_{11}),$$

in which the coefficients δ_n are defined in Table 2.

Table 2. The HRS first hyperpolarizability coefficients (δ_n).

$\delta_1 = \sum_i \beta^2_{iii}$	$\delta_2 = \sum_{i,j} \beta_{iii}\beta_{ijj}$	$\delta_3 = \sum_{i,j} \beta_{iii}(\beta_{jij} + \beta_{jji})$
$\delta_4 = \sum_{i,j} \beta^2_{ijj}$	$\delta_5 = \sum_{i,j} \beta_{ijj}(\beta_{iij} + \beta_{jii})$	$\delta_6 = \sum_{i,j} (\beta_{jij} + \beta_{jji})^2$
$\delta_7 = \sum_{i,j,k} \beta_{ijj}\beta_{ikk}$	$\delta_8 = \sum_{i,j,k} (\beta_{iij} + \beta_{jji})(\beta_{kik} + \beta_{kki})$	$\delta_9 = \sum_{i,j,k} \beta_{ijj}(\beta_{kik} + \beta_{kki})$
$\delta_{10} = \sum_{i,j,k} (\beta_{ijk} + \beta_{ikj})^2$	$\delta_{11} = \sum_{i,j,k} (\beta_{ijk} + \beta_{ikj})(\beta_{jjk} + \beta_{jki})$	

Using the Kleymann symmetry, the average value of the second hyperpolarizability (γ) can be calculated through the following expression,

$$\langle\gamma\rangle = \frac{1}{5}[\gamma_{xxxx} + \gamma_{yyyy} + \gamma_{zzzz} + 2(\gamma_{xxyy} + \gamma_{xxzz} + \gamma_{yyzz})] \qquad (5)$$

The linear and nonlinear optical (NLO) parameters of the molecules of chalcone derivatives in several solvent media were calculated using the PCM/DFT/CAM-B3LYP/6-311+G(d) level with the Gaussian 09 software package.

Results and Discussion

Solvent effects on the molecular properties

In this section, the similarities between the molecular geometry of 4MP3P and 4NP3P, obtained via X-ray diffraction [15, 16], and the theoretical results in several solvent media are analyzed through the root mean square deviation (RMSD) of the overlap of the two structures. As can be seen, in Table 3, the value of RMSD is 0.156 a.u. (0.217 a.u.) for gas phase of 4MP3P (4NP3P) and this value presents small changes when the solvent dielectric constant increases, until reaching the value 0.167 a.u. (0.295 a.u.), therefore the effects of solvent media on the molecular geometry is more significant for 4NP3P. Figure 2 shows a schematic representation of the overlap of 4MP3P and 4NP3P molecular structure determined by X-ray (in blue) and in water (in red), where the phenyl ring (A) was used as anchorage for the molecular structures. The H-atoms were disregarded in view of their uncertainties in X-ray position refinement.

Table 3. RMSD (a.u.) and Gap energies (eV) of 4MP3P and 4NP3P.

Solvent	ε	RMSD 4MP3P	RMSD 4NP3P	Gap (eV) 4MP3P	Gap (eV) 4NP3P
Gas-phase	1.00	0.156	0.217	6.636	6.094
Heptane	1.91	0.158	0.285	6.587	5.980
Chloroform	4.71	0.162	0.292	6.537	5.886
Tetrahydrofuran	7.43	0.163	0.293	6.520	5.859
Dichloroethane	10.13	0.164	0.294	6.511	5.846
Acetone	20.49	0.165	0.295	6.499	5.829
Ethanol	24.85	0.166	0.295	6.496	5.825
Methanol	32.61	0.166	0.295	6.494	5.822
DMSO	46.71	0.166	0.295	6.491	5.819
Water	78.36	0.167	0.295	6.489	5.815

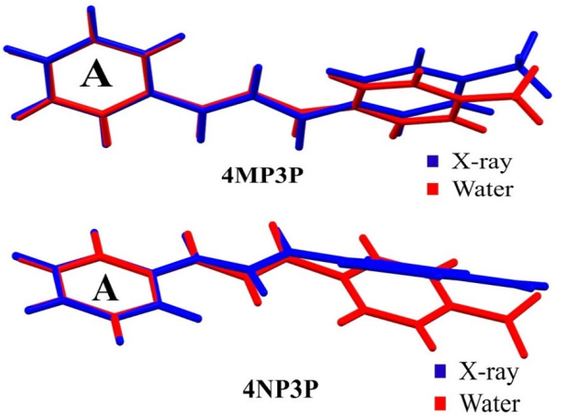

Figure 2. Overlap of the theoretical molecular structures of the compounds (4MP3P and 4NP3P) in water (red) and that determined by X-ray diffraction (blue).

Table 4 shows the (O1-C9-C8-C7), (C8-C9-C10-C11), (C8-C9-C10-C15), (C8-C7-C6-C5), (C8-C7-C6-C5), and (01-C9-C10-C15) torsion angles for various solvents and for the gas-phase. As can be seen, the torsion angles present a small variations in all solvent media, independent of the solvent polarity or the protic or aprotic character for both compunds 4MP3P and 4NP3P.

The results of the solvent torsion angles as compared with the gas–phase present a small variation in their absolute values and for 4NP3P a signal inversion occurs. In addition, in Table 4 the X-ray results for the torsion angles for the compounds in crystalline phase are presented. Comparing these angles with the results obtained in gas-phase one can see that greater differences occur for 4NP3P, whose variations can reach 27°.

Table 4. Geometrical parameters related to torsion angle (º).

	O1-C9-C8-C7		C8-C9-C10-C11		C8-C9-C10-C15		C8-C7-C6-C1		C8-C7-C6-C5		01-C9-C10-C15	
	4MP3P	4NP3P	4MP3P	4NP3P	4MP3P	4NP3P	4MP3P	4NP3P	4MP3P	4NP3P	4MP3P	4NP3P
X-Ray	17.83	0.54	6.84	-5.8	-176.07	176,00	-179.29	-171.29	2.25	8.14	3.97	-4.37
Gas-Phase	5.86	5.86	14.09	20.69	-167.3	-160.95	-176.61	-177.11	3.66	2.97	12,00	18.22
Heptane	6.18	-5.84	15,00	-22.4	-166.42	159.3	-176.95	176.91	3.19	-3.17	12.87	-19.85
Chloroform	6.44	-5.7	15.79	-23.51	-165.65	158.2	-177.27	177.29	2.84	-2.75	13.62	-20.98
Tetrahydrofuran	6.5	-5.66	16.03	-23.83	-165.41	157.88	-177.37	177.56	2.74	-2.47	13.85	-21.31
Dichloroethane	6.52	-5.65	16.14	28.98	-165.29	157.72	-177.42	177.64	2.69	-2.38	13.96	-21.48
Acetone	6.55	-5.62	16.32	-24.23	-165.1	157.45	-177.51	177.93	2.59	-2.07	14.14	-21.75
Ethanol	6.56	-5.61	16.36	-24.28	-165.06	157.4	-177.53	178,00	2.57	-2.01	14.17	-21.8
Methanol	6.56	-5.61	16.4	-24.33	-165.02	157.35	-177.55	178.07	2.55	-1.92	14.21	-21.86
DMSO	6.57	-5.59	16.44	-24.39	-164.97	157.29	-177.57	178.15	2.53	-1.84	14.25	-21.92
Water	6.57	-5.58	16.49	-24.44	-164.93	157.23	-177.59	178.23	2.51	-1.76	14.29	-21.98

Table 5. Geometrical parameters related to angle (º).

	O1-C9-C8		C8-C9-C10		C8-C7-C6		N1-C13-C14	N1-C13-C12	C16-C13-C14	C16-C13-C12
	4MP3P	4NP3P	4MP3P	4NP3P	4MP3P	4NP3P	4NP3P	4NP3P	4MP3P	4MP3P
X-ray	119.97	121.21	120.19	120.21	128.41	127.52	117.79	119.33	120.92	121.68
Gas-Phase	121.07	122.11	119.94	118.82	127.95	129.07	119,00	118.86	120.71	121.32
Heptane	121.15	122.33	118.95	118.68	127.91	128.01	118.97	118.86	120.72	121.32
Chloroform	121.23	122.49	118.89	118.58	127.85	127.94	118.93	118.86	120.72	121.31
Tetrahydrofuran	121.25	122.54	118.88	118.35	127.83	127.92	118.91	118.87	120.73	121.3
Dichloroethane	121.26	122.56	118.87	118.54	127.81	127.9	118.9	118.87	120.73	121.39
Acetone	121.28	122.59	118.56	118.51	127.79	127.88	118.89	118.87	120.73	121.29
Ethanol	121.28	122.6	118.86	118.51	127.79	127.87	118.89	118.87	120.73	121.29
Methanol	121.29	122.6	118.86	118.51	127.78	127.87	118.89	118.87	120.73	121.29
DMSO	121.29	122.61	118.86	118.5	127.78	127.96	118.88	121.29	120.73	121.29
Water	121.29	122.62	118.86	118.5	127.78	127.86	118.88	118.88	120.73	121.29

Results for the angles (O1-C9-C8), (C8-C9-C10), (C8-C7-C6) for both compounds and the angles (N1-C13-C14) and (N1-C13-C12) for 4NP3P, and the angles (C16-C13-C14) and (C16-C13-C12) for 4MP3P are presented in Table 5. As can be seen, the results for these angles presents no significative variation caused by the presence of the solvent media.

The asymmetric distribution of electrons in the chemical bonds of the molecular compounds can be visualized by the partial charges calculations in gas-phase. For 4MP3P the total charges of the groups (C4-C5-C6-C7-C8-C9-C16-H3-H4-H5-H6-H12-H13-H14), (C10-C11-C12-C13-C14-C15-H7-H8-H9-H10-H11), and (C1-C2-C3-H1-H2-O1) are 0.012 e, 0.148 e and -0.159 e, respectively. For 4NP3P the total charges of the (C10-C15-H15-C14-H14-C13-C12-H12-C11-H11), (C1-H1-C2-H2-C3-H3-C4-H4-C5-H5-C6), (C7-H7-C8-H8-C9-H9-O1), and (N1-O2-O3) are 0.170 e, 0.152 e, -0.101 e and -0.221 e, respectively. The transfer of charge is greater for the polar solvent media than that for the nonpolar solvent *(ε<5)*.

The gap energy (E_G) calculated from the difference between the HOMO and LUMO energies is also shown in Table 3 for several solvent media. As can be noted, the substituent change, from CH_3 (4MP3P) by the NO_2 (4NP3P), causes a decreasing (~11%) in the gap energy in all solvent media.

Figure 3 shows the HOMO and LUMO orbitals for 4MP3P and 4NP3P in water, presenting the lowest values of gap energy. Also it shows that the smaller the value of gap energy the better the nonlinear optical properties of the compound [7]. Both HOMO and LUMO present π-bonds.

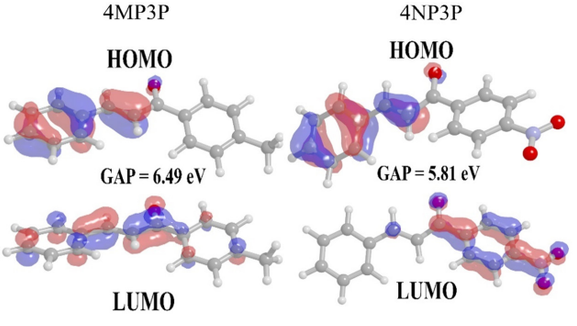

Figure 3. Frontiers orbital HOMO and LUMO for 4MP3P and 4NP3P in water.

Nonlinear optical properties

Table 6 shows the DFT/CAM-B3LYP/6-311+G(d) results for the dipole moment (μ) in debye units (D) for both compounds in the gas-phase and in various solvents. As can be seen the μ-value increases with the increasing of the ε-value. For 4MP3P (4NP3P) the dipole moment increases 48.5% (23.6%) as compared with the gas-phase. As example, in water the substituent changes from 4-methylphenyl to 4-nitrophenyl increases the μ-value of 62.5%, evidencing a greater negative charge transfer for the NO_2 group.

The behavior of the static values of the average linear polarizability (<α(0,0)>) first hyperpolarizability (<$\beta_{\|}$(0,0,0)>) and average second hyperpolarizability (<γ(0,0,0,0)>) as function of ε-values for both compounds are shown in the Table 7. As can be seen, all absolute values of these parameters increase when the ε-values for both compounds also increase, the result being greater for 4NP3P. Comparing the absolute values of these parameters for 4MP3P with those for 4NP3P,we can see that the static linear polarizability exhibits the smallest variation (~3%) and the absolute values of the parallel first hyperpolarizability present the greatest variation (more than 150%). So, the substituent change benefits the nonlinear optical properties of the compounds; this fact can be seen for the <γ(0,0,0,0)>-value that is greater (~20%) for 4NP3P than for 4MP3P, showing that accumulation of negative charges in the NO_2 group favors the electron cloud distortion.

Table 6. Dipole moment values (D) for 4MP3P and 4NP3P in several solvent media.

Solvent	ε	4MP3P	4NP3P
Gas-phase	1	3.34	6.52
Heptane	1.91	3.84	7.12
Chloroform	4.71	4.39	7.64
Tetrahydrofuran	7.43	4.58	7.79
Dichloroethane	10.13	4.68	7.87
Acetone	20.49	4.84	7.98
Ethanol	24.85	4.86	8.00
Methanol	32.61	4.89	8.02
DMSO	46.7	4.92	8.05
Water	78.36	4.96	8.06

Table 7. Static values of the average linear polarizability (in 10^{-24} esu), first hyperpolarizability (in 10^{-30} esu) and average second hyperpolarizability (in 10^{-36} esu) for 4MP3P and 4NP3P.

Solvent	4MP3P	4NP3P	4MP3P	4NP3P	4MP3P	4NP3P
	$\alpha(0;0)$	$\alpha(0;0)$	$\beta_{\|\|}z(0;0,0)$	$\beta_{\|\|}z(0;0,0)$	$\gamma_{\|\|}(0;0,0,0)$	$\gamma_{\|\|}(0;0,0,0)$
Gas-phase	30.80	31.72	-4.58	-13.81	61.03	69.70
Heptane	34.37	35.46	-7.19	-21.11	91.54	108.10
Chloroform	38.14	39.40	-10.69	-29.60	131.53	158.49
Tetrahydrofuran	39.42	40.73	-12.04	-32.56	146.95	177.54
Dichloroethane	40.09	41.42	-12.77	-34.09	155.30	187.70
Acetone	41.11	42.46	-13.92	-36.41	168.51	203.57
Ethanol	41.29	42.65	-14.13	-36.84	170.98	206.51
Methanol	41.51	42.87	-14.38	-37.32	173.84	209.90
DMSO	41.72	43.09	-14.62	-37.80	176.69	213.29
Water	41.92	43.29	-14.86	-38.25	179.41	216.49

Table 8. Static and dynamic values of the HRS first hyperpolarizabilities (in 10^{-30} esu) for 4MP3P and 4NP3P.

		4MP3P	4NP3P	4MP3P	4NP3P
		$\beta_{HRS}(0;0,0)$	$\beta_{HRS}(0;0,0)$	$\beta_{HRS}(-2\omega;\omega,\omega)$	$\beta_{HRS}(-2\omega;\omega,\omega)$
Gas-phase	1	5.208	9.754	7.644	19.426
Heptane	1.91	7.985	14.755	12.212	30.997
Chloroform	4.71	11.622	20.583	14.124	35.754
Tetrahydrofuran	7.43	13.003	22.615	14.253	36.048
Dichloroethane	10.13	13.742	23.665	14.863	37.448
Acetone	20.49	14.900	25.264	14.419	36.352
Ethanol	24.85	15.115	25.555	14.508	36.544
Methanol	32.61	15.363	25.888	14.250	35.924
DMSO	46.7	15.611	26.219	15.210	38.145
Water	78.36	15.846	26.530	14.438	36.328

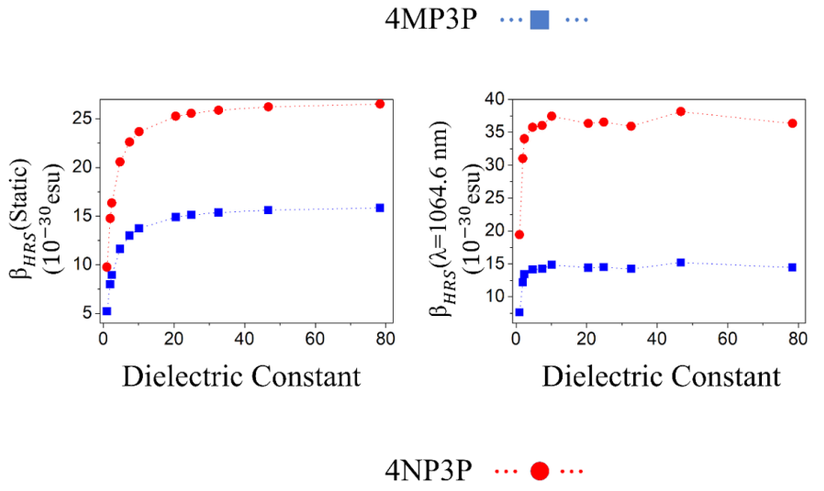

Figure 4. Static and dynamic HRS first-hyperpolarizabilities as function of the dielectric constant values.

The increasing of the α(0;0)-values is greater for the nonpolar solvents (~14%) than for the aprotic (~4%) and protic (~1.5%) solvents for both compounds. However, the increasing of the static absolute β-values and γ-values are basically the same for both 4MP3P and 4NP3P, in protic solvents around of 5%, in aprotic solvents around of ~14% and for nonpolar solvents around 60%. These results show that for the nonpolar solvents the dielectric properties of the medium are the strongest characteristic to be considered, but for the aprotic and protic solvents considered here, despite the great increasing of values of the solvent dielectric constant between then, the effect on the electric parameters is small.

Table 8 shows the static and dynamic (ω=0.0428 a.u.) results for HRS hyperpolarizabilities (β_{HRS}) as function of the dielectric constant value; as can be seen, the β_{HRS}(0;0,0)-value increases when the ε-value also increases. The highest values of the static-β_{HRS} occur in water $26.53 \cdot 10^{-30}$ esu and $15.846 \cdot 10^{-30}$ esu for 4NP3P and 4MP3P, respectively, indicating a significant difference of 67% due the substituent change at position 4 of the phenyl ring. The highest values of the dynamic β_{HRS}(-2ω;ω,ω) occur in DMSO, namely $15.21 \cdot 10^{-30}$ esu (4MP3P) and $38.145 \cdot 10^{-30}$ esu (4NP3P).

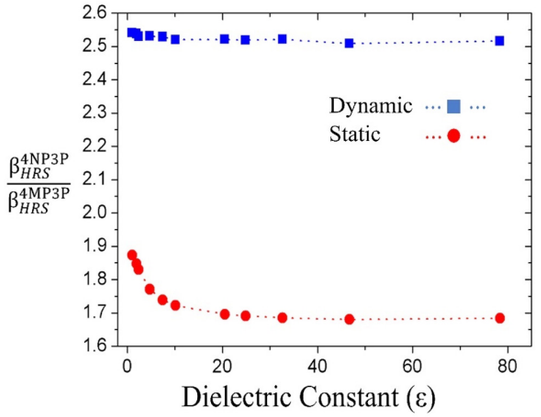

Figure 5. βHRS-ratio for the compounds 4MP3P and 4NP3P as function of ε for the static and dynamic (ω = 0.428 a.u) cases.

In Figure 4, for the two chalcone derivatives, the static and dynamic results for β_{HRS} are plotted as function of the ε-values; as we can observe, the values for 4NP3P are greater than those of 4MP3P.

The β_{HRS}-ratio between the compounds 4NP3P (β_{HRS}^{4NP3P}) and 4MP3P (β_{HRS}^{4MP3P}) as function of ε for the dynamic (ω = 0.0428 a.u) and static case are shown in Figure 5. As can be seen, in the dynamic case, the β_{HRS}-ratio is around 2.5 and for the static case the value lies between 1.7 and 1.9.

Conclusions

We have reported the geometrical and nonlinear optical properties of two chalcone derivatives: (*E*)-1-(4-methylphenyl)-3-phenylprop-2-en-1-one (4MP3P) and (*E*)-1-(4-Nitrophenyl)-3-phenylprop-2-en-1-one (4NP3P), within the DFT/CAM-B3LYP/6-311+G(d) level. The effects of the various solvents on the electrical parameters of the two chalcone derivatives were considered via the Polarizable Continuum Model (PCM). The values of the dipole moment (μ) increase with the increasing of the solvent dielectric constant values and this increasing is greater for 4MP3P than for 4NP3P. However, the substituent change of CH_3 to NO_2 increases the μ-value for all solvents; as an example, in water this increase is of 62.5%, evidencing the greater negative charge transfer for the NO_2 group. The static linear polarizability presents the smaller variation (~3%) due to the solvent medium presence; however, the absolute values of the parallel first hyperpolarizability present the greater variation (more than 150%). Therefore, the substituent change of CH_3 (4MP3P) to NO_2 (4NP3P) benefits the nonlinear optical properties of the compounds. The HRS hyperpolarizability (β_{HRS}) as function of the solvent dielectric constant value were calculated as in static and dynamic cases. The static β_{HRS}-values also increase when the ε-value increases. The highest values of the static-β_{HRS} occur in water $26.53 \cdot 10^{-30}$esu and $15.846 \cdot 10^{-30}$esu for 4NP3P and 4MP3P, respectively, indicating a significant difference of 67% due the substituent change.

Acknowledgements

The authors would like to thank the partial supports of the following Brazilian agencies: Conselho Nacional de Desenvolvimento Científico e Tecnológico (CNPq), Coordenação de Aperfeiçoamento Pessoal de Nível Superior (CAPES); Pró-Reitoria de Pesquisa e Pós-Graduação da PUC-GO (Prope) e Fundação de Apoio Pesquisa do Estado de Goiás (FAPEG). Research developed with support from the High Performance Computing Center at Universidade Estadual de Goiás (UEG).

References

[1] M. Anis, G. G. Muley, V. G. Pahurkar, M. I. Baig, and S. R. Dagdale, "Influence of Nd 3+ on zinc tris-thiourea sulphate single crystal: a comparative crystal growth, structural, linear–nonlinear optical and dielectric study to explore NLO device applications", *Mater. Res. Innov.*, vol. 22, no. 2, pp. 99–106, 2018. DOI: https://doi.org/10.1080/14328917.2016.1264848.

[2] X. Fan *et al.*, "Broken Symmetry Induced Strong Nonlinear Optical Effects in Spiral WS 2 Nanosheets," *ACS Nano*, vol. 11, no. 5, pp. 4892–4898, 2017. DOI: https://doi.org/10.1021/acsnano.7b01457.

[3] P. K. Johansson, L. Schmüser, and D. G. Castner, "Nonlinear Optical Methods for Characterization of Molecular Structure and Surface Chemistry," *Top. Catal.*, vol. 61, no. 9–11, pp. 1101–1124, 2018. DOI: https://doi.org/10.1007/s11244-018-0924-3.

[4] L. Lu *et al.*, "Few-layer Bismuthene: Sonochemical Exfoliation, Nonlinear Optics and Applications for Ultrafast Photonics with Enhanced Stability", Laser Photon. Rev., vol. 12, no. 1, p. 1700221, 2018. DOI: https://doi.org/10.1002/lpor.201700221.

[5] M. Luo *et al.*, "M 2 B 10 O 14 F 6 (M = Ca, Sr): Two Noncentrosymmetric Alkaline Earth Fluorooxoborates as Promising Next-Generation Deep-Ultraviolet Nonlinear Optical Materials", *J. Am. Chem. Soc.*, vol. 140, no. 11, pp. 3884–3887, 2018. DOI: https://doi.org/10.1021/jacs.8b01263.

[6] A. N. Castro *et al.*, "Theoretical study on the third-order nonlinear optical properties and structural characterization of 3-Acetyl-6-Bromocoumarin," *Chem. Phys. Lett.*, vol. 653, pp. 122–130, 2016. DOI: https://doi.org/10.1016/j.cplett.2016.04.070.

[7] A. N. Castro, F. A. P. Osório, R. R. Ternavisk, H. B. Napolitano, C. Valverde, and B. Baseia, "Theoretical investigations of nonlinear optical properties of two crystalline acetamides structures including polarization effects of their environment", *Chem. Phys. Lett.*, vol. 681, pp. 110–123, 2017. DOI: https://doi.org/10.1016/j.cplett.2017.05.066.

[8] T. Chandra Shekhara Shetty, S. Raghavendra, C. S. Chidan Kumar, and S. M. Dharmaprakash, "Nonlinear absorption, optical limiting behavior and structural study of a new chalcone derivative-1-(3, 4-dimethylphenyl)-3-[4(methylsulfanyl) phenyl] prop-2-en-1-one", *Opt. Laser Technol.*, vol. 77, pp. 23–30, 2016. DOI: https://doi.org/10.1016/j.optlastec.2015.08.015.

[9] S. Bag *et al.*, "Design, synthesis and biological activity of multifunctional α,β-unsaturated carbonyl scaffolds for Alzheimer's disease", *Bioorg. Med. Chem. Lett.*, vol. 23, no. 9, pp. 2614–2618, 2013. DOI: https://doi.org/10.1016/j.bmcl.2013.02.103.

[10] Y. Wang, S. Xue, R. Li, Z. Zheng, H. Yi, and Z. Li, "Synthesis and biological evaluation of novel synthetic chalcone derivatives as anti-tumor agents targeting Cat L and Cat K", *Bioorg. Med. Chem.*, vol. 26, no. 1, pp. 8–16, 2018. DOI: https://doi.org/10.1016/j.bmc.2017.09.019.

[11] J. Li *et al.*, "Design, synthesis, biological evaluation, and molecular docking of chalcone derivatives as anti-inflammatory agents", *Bioorg. Med. Chem. Lett.*, vol. 27, no. 3, pp. 602–606, 2017. DOI: https://doi.org/10.1016/j.bmcl.2016.12.008.

[12] D. Choi *et al.*, "In Vitro Osteogenic Differentiation and Antibacterial Potentials of Chalcone Derivatives", *Mol. Pharm.*, vol. 15, no. 8, pp. 3197–3204, 2018. DOI: https://doi.org/10.1021/acs.molpharmaceut.8b00288.

[13] L. Illicachi *et al.*, "Synthesis and DFT Calculations of Novel Vanillin-Chalcones and Their 3-Aryl-5-(4-(2-(dimethylamino)-ethoxy)-3-methoxyphenyl)-4,5-dihydro-1H-pyrazole-1-carbaldehyde Derivatives as Antifungal Agents", *Molecules*, vol. 22, no. 9, p. 1476, 2017. DOI: https://doi.org/10.3390/molecules22091476.

[14] L. M. G. Abegão *et al.*, "Second- and third-order nonlinear optical properties of unsubstituted and mono-substituted chalcones", *Chem. Phys. Lett.*, vol. 648, pp. 91–96, 2016. DOI: https://doi.org/10.1016/j.cplett.2016.02.009.

[15] F. Toda, K. Tanaka, and M. Kato, "Stereoselective photodimerisation of chalcones in the molten state", *J. Chem. Soc. Perkin Trans. 1*, no. 7, pp. 1315–1318, 1998. DOI: https://doi.org/10.1039/a707380a.

[16] L.-H. Jing, "(E)-1-(4-Nitrophenyl)-3-phenylprop-2-en-1-one", *Acta Crystallogr. Sect. E Struct. Reports Online*, vol. 65, no. 10, pp. o2510–o2510, 2009. DOI: https://doi.org/10.1107/S1600536809037556.

[17] C. Laane, S. Boeren, K. Vos, and C. Veeger, "Rules for optimization of biocatalysis in organic solvents", *Biotechnol. Bioeng.*, vol. 30, no. 1, pp. 81–87, 1987. DOI: https://doi.org/10.1002/bit.260300112.

[18] W. J. Geary, "The use of conductivity measurements in organic solvents for the characterisation of coordination compounds", *Coord. Chem. Rev.*, vol. 7, no. 1, pp. 81–122, 1971. DOI: https://doi.org/10.1016/S0010-8545(00)80009-0.

[19] C. Valverde, Í. N. Ribeiro, J. V. B. Soares, B. Baseia, and F. A. P. Osório, "Prediction of the Linear and Nonlinear Optical Properties of a Schiff Base Derivatives via DFT", *Adv. Condens. Matter Phys.*, vol. 2019, pp. 1–12, 2019. DOI: https://doi.org/10.1155/2019/8148392.

[20] S. Backus *et al.*, "16-fs, 1-μJ ultraviolet pulses generated by third-harmonic conversion in air", *Opt. Lett.*, vol. 21, no. 9, p. 665, 1996. DOI: https://doi.org/10.1364/OL.21.000665.

[21] J. M. F. Custodio *et al.*, "Chalcone as Potential Nonlinear Optical Material: A Combined Theoretical, Structural, and Spectroscopic Study", *J. Phys. Chem. C*, vol. 123, no. 10, pp. 5931–5941, 2019. DOI: https://doi.org/10.1021/acs.jpcc.9b01063.

[22] C. Reichardt, *Solvents and Related Titles from WILEY-VCH Organic Synthesis Workbook II Chemical Synthesis Using Supercritical Fluids*. 2003.

Article citation:
J. V. B. Soares, C. Valverde, A. D. da Silva, B. V. Luz, D. J. A. dos Santos, E. G. B. Carvalho, Y. C. M. Oliveira, H. B. Napolitano, B. Baseia & F. A. P. Osório. "Theoretical study of solvent effects on the hyperpolarizabilities of two chalcone derivatives" *Rev. Colomb. Quim.*, vol. 49, no. 1, pp. 33-39, 2020. DOI: http://dx.doi.org/10.15446/rev.colomb.quim.v1n49.69474